Chapter 11

Prolactin Receptor Isoforms in Human Breast Cancer

Erika Ginsburg, Christopher D. Heger, Paul Goldsmith and Barbara K. Vonderhaar

Additional information is available at the end of the chapter

http://dx.doi.org/10.5772/54217

1. Introduction

Prolactin (PRL) is a polypeptide hormone secreted by the anterior pituitary responsible for the growth and differentiation of the normal mammary gland and plays a role in breast cancer. It functions systemically as an endocrine factor, but PRL may also act in an autocrine/paracrine fashion in a number of other tissues. Studies in both pre- and post-menopausal women have determined a significant increased risk for breast cancer for those with serum PRL in the highest quartile [6, 7]. PRL, acting through its receptors, has been shown to increase cell proliferation and decrease apoptosis in breast cancer cells *in vitro* [3, 8]. PRL also acts as a pro-angiogenic factor in mammary tissues [9]. PRL exerts its effects by binding to its receptors on the surface of normal human breast epithelial and cancer cells, initiating the Jak2/Stat5, PI3K, and mitogen-activated protein kinase (MAPK) signaling pathways [3].

The PRL receptor (PRLR) is a member of the class I cytokine/hematopoietic receptor superfamily. A single hydrophobic transmembrane region separates the extracellular ligand-binding domain from the intracellular signaling domain. Five cell-associated PRLR isoforms differ only in their C-terminal cytoplasmic domains [1, 3]. The three major isoforms (long, LF; short 1a and 1b, SF1a and SF1b, respectively) are regulated by PRL itself. LF signals for many functions including growth and differentiation, whereas SF1a and SF1b act as dominant-negatives for differentiation [1, 2]. The role of the short forms in breast cell growth remains to be determined.

2. Problem statement

Studies from our laboratory [1] and from others [2] have demonstrated that three specific isoforms of the PRLR are expressed in both normal and cancerous breast cells and tissues. We recently developed and characterized PRLR isoform specific polyclonal antibodies that

revealed that the three isoforms, LF, SF1a, and SF1b, are differentially expressed in ductal and lobular carcinomas [5]. These two most common histological types of breast cancer originate from the terminal ductal lobular unit and may be difficult to classify. However, distinct differences were observed in PRLR expression in normal, benign, and malignant breast tissue which may have prognostic significance [10, 11]. The development and characterization of PRLR isoform specific monoclonal antibodies will provide a near limitless supply of reagent to continue to examine how and where these isoforms interact both in normal breast development and in breast cancer.

3. Application area

The identification of estrogen receptor (ER) and progesterone receptor (PR) in the current testing of breast cancer has advanced the field. Other hormones/growth factors are also involved; for example, PRL and its receptor isoforms. If their roles are more clearly identified with the use of specific antibodies then there may be a practical need for them in the diagnosis of this disease. Examining normal breast development could give clues to the relevance of PRLR isoforms in cancer. Not only do these apply to the breast, but may also be of value to studying ovarian and prostate cancers where PRL may play a role/function. PRLR isoform specific antibodies could be powerful tools in this quest.

4. Methods

4.1. Preparation of the PRLR isoform specific monoclonal antibodies

Synthetic peptides were designed based on the regions of unique intracellular sequences of the PRLR splice variants and synthesized (AnaSpec, Inc., San Jose, CA) by the solid-phase method. Peptides (4 mg) were conjugated to bovine serum albumin (10 mg) with 1mM DSS overnight at room temperature and sent to Epitomics (Burlingame, CA) for immunization of rabbits. Initially, a total of 76 clones were received (54 clones for SF1a, 22 clones for SF1b) and screened for reactivity to their respective antigens by Western blot analysis. Briefly, lysates of CHO-K1 cells expressing either SF1a or SF1b were separated by SDS-PAGE, and transferred to PVDF. Membranes were blocked for 1 hr at room temperature in 5% non-fat dairy milk diluted in TBST+0.1% sodium azide. Subsequently, the clonal supernatants were diluted 1:1 in 10% non-fat dairy milk (diluted in TBST+0.1% sodium azide) and incubated for 3 hr at room temperature. Membranes were washed and probed with goat anti-rabbit Alexa680 (1:4000) prior to visualization using a LiCOR Odyssey reader. Supernatants from positively reacting clones were re-screened prior to selection for subcloning. In total, four SF1a and six SF1b rabbit monoclonal antibodies were put into production. The rabbit sera were initially purified by MEP Hypercel (PAL) chromatography, followed by size-exclusion chromatography to further purify the antibodies. Final pools of antibody were produced and protein concentration determined by the Pierce 660nm assay.

For LF, 6 mg peptide was conjugated to 3 mg keyhole limpet hemocyanin overnight at room temperature using glutaraldehyde. Peptide conjugates were sent to Green Mountain

Antibodies (Burlington, VT) for generation of mouse monoclonal antibodies. Initially, 120 clones were screened by Western blot as described above using CHO-K1 cells expressing LF with the exception that the antibodies were diluted 1:100 in 5% non-fat dairy milk (diluted in TBST+0.1% sodium azide) and incubated overnight at 4° C. Secondary antibody and imaging were essentially as described above. Supernatants of positively reacting clones were re-screened by Western blot and examined by fluorescence microscopy (to confirm appropriate localization) prior to selection for production. In total, 10 positive clones were selected for this process, 8 of which produced IgG. Antisera was purified as described for SF1a and SF1b antibodies. Final pools of antibody were produced and protein concentration determined by the Pierce 660nm assay.

4.2. Cell culture and transfection

Chinese hamster ovary cells (CHO-K1, ATCC, Manassas, VA) were maintained in α-MEM (Invitrogen, Gaithersburg, MD) supplemented with 5% fetal bovine serum (FBS, Invitrogen) and penicillin/streptomycin (100 U/ml and 100 μg/ml respectively, Invitrogen). Transfections were performed using FuGENE 6 (Roche Applied Science, Indianapolis, IN) at a ratio of 1 μg DNA to 3 μl FuGENE. The PRLR isoform specific cDNA constructs were previously described [1]. Cells were transfected for 48 hr, then allowed to grow for an additional 48 hr.

T47D, ZR75-1, MDA-MB-231, MDA-MB-468, MCF7, and SK-BR-3 breast cancer cell lines were obtained from ATCC. T47D, ZR75-1, MDA-MB231, and MDA-MB468 cells were maintained in RPMI1640 (Invitrogen). MCF7 cells were grown in DMEM and SK-BR-3 cells were maintained in McCoys 5a media. All media were supplemented with 5% heat inactivated FBS, 10 μg/ml bovine insulin (Sigma, St. Louis, MO), and penicillin-streptomycin (100 U/ml and 100 μg/ml respectively, Invitrogen). Where indicated, breast cancer cell lines were plated on 8-well glass chamber slides (Nunc, Rochester, NY) in normal growth media, and allowed to attach overnight. The media were replaced and the cells were treated for the indicated times with 500 ng/ml recombinant human PRL in media where the FBS was replaced with 1% charcoal stripped serum, then fixed in 10% normal buffered formalin prior to Duolink assay.

All cells were maintained at 37 °C in a humidified atmosphere with 5% CO2. Cells were passaged using trypsinization (0.05% trypsin-EDTA, Invitrogen) and counted on a hemocytometer using trypan blue exclusion

4.3. Western blot analysis

Transfected CHO cells were collected and whole cell lysates were prepared in Complete Buffer (Roche Applied Science) according to the manufacturer's instructions. Total protein was estimated according to Bradford [12]. Protein (100 μg) was subjected to 10-20% SDS-PAGE (Invitrogen). Proteins were transferred to nitrocellulose membrane and probed with PRLR isoform specific antibodies (10 μg/ml for LF, 6 μg/ml for SF1a or SF1b). Reactivity was detected using ECL Plus (GE Healthcare Life Science, Pittsburgh, PA). Molecular size determinations were made using BenchMark Protein Ladder (Invitrogen).

4.4. Fluorescent immunocytochemistry

CHO cells were plated on 8-well glass chamber slides (Nunc) and transfected as above. After blocking with 5% normal goat serum (Jackson Laboratories, Bar Harbor, ME) prepared in PBS-0.1% Triton, slides were incubated with the PRLR isoform specific monoclonal antibodies (10 μg/ml for LF, 6 μg/ml for SF1a or SF1b) overnight at 4° C. In all cases no primary antibody served as the negative control. Slides were washed four times with PBS-0.1% Triton followed by incubation for 1 hr with either red fluorescent tagged goat anti-mouse secondary antibody for the PRLR-LF or red fluorescent tagged goat anti-rabbit secondary antibody for the PRLR-SF (AlexaFluor 594, 1:500, Invitrogen) in the dark. After extensive washing with PBS containing Triton, slides were mounted with Prolong Gold antifade reagent with DAPI (Invitrogen). The fluorescent staining pattern of the receptor isoforms was evaluated using an Olympus BX40 fluorescence microscope (Olympus America, Center Valley, PA).

4.5. Fluorescent immunohistochemistry

Fresh breast samples were supplied by either the Cooperative Human Tissue Network, a NCI supported resource that supplies human biospecimens to IRB approved researchers, or from patient samples collected in accordance with the guidelines of the National Cancer Institute Review Board, protocol 02-C-0144. Breast tissue was obtained from 15 pre-menopausal reduction mammoplasty patients; each sample was determined free from hyperplastic growth by a pathologist. Samples were fixed in 10% normal buffered formalin, embedded, cut into four micron sections, deparaffinized, and stained as above. For dual labeling studies, sections were incubated overnight at 4° C with LF (10 μg/ml) and either SF1a or SF1b (6 μg/ml) monoclonal antibodies. Red fluorescent anti-mouse secondary antibody (AlexaFluor 594, 1:500) was used for LF; green fluorescent anti-rabbit secondary antibody (AlexaFluor 588, 1:500) was used for SF1a and SF1b.

An additional eight samples were also snap-frozen and stored at -80° C for OCT embedding and sectioning. Frozen tissue sections were thawed for 30 to 60 sec and fixed in ice-cold methanol:acetone (1:1) for 10 min. After washing twice with PBS, sections were blocked for 30 min with 10% normal goat serum in IF buffer (PBS containing 0.05 mg/ml sodium azide, 0.1 mg/ml BSA, 0.02% Triton X, and 0.05% Tween 20). Sections were incubated with either LF (10 μg/ml) and SF1a or SF1b (6 μg/ml) PRLR isoform specific monoclonal antibodies overnight at 4° C. Sections were extensively washed with PBS, then incubated with red fluorescent anti-mouse secondary antibody (AlexaFluor 594, 1:500) for LF and green fluorescent anti-rabbit secondary antibody (AlexaFluor 588, 1:500) for SF1a and SF1b. Sections were washed again and mounted with Prolong Gold antifade reagent with DAPI.

The fluorescent staining patterns of the PRLR isoforms were assessed using an Olympus BX40 fluorescent microscope. For both paraffin-embedded and frozen tissue sections, photographs were immediately taken under the violet, green, and blue channels to detect DAPI, red, and green fluorescence, respectively. Images were merged in order to observe PRLR isoform localization patterns.

Nine samples of paraffin-embedded breast tumor tissue were stained and analyzed as above.

4.6. Measurement of fluorescence intensity

Because serial sections for the breast specimens were used, the same region of each tissue could be measured for fluorescence intensity using Adobe Photoshop (Adobe Systems Inc., Beaverton, OR). Nearly every cell in positive samples showed some level of PRLR isoform expression; as a result, red fluorescence intensity was used to compare levels of isoform expression between samples. In order to do this, the same fluorescent areas were selected from each serial section using the lasso and rectangular marquee tools. Selected sections were analyzed using the histogram function through the red channel, which gave the mean red intensity of the selected section. Photoshop assigns intensity values between 0 and 255 to each pixel in the selected area and then averages these intensities. The distribution of these means was analyzed and used to divide samples into four intensity classes: negative (less than 10 intensity), low (between 11 and 30 intensity), medium (between 31 and 50 intensity), and high (greater than 51 intensity).

4.7. Generation of ProbeMaker probes for Duolink

Antibodies against the various PRLR isoforms were directly conjugated using the ProbeMaker protocol as described by the manufacturer (OLINK BioScience, Upsala, Sweden). Briefly, 2 μl ProbeMaker conjugation buffer was added to 20 μg of each antibody (starting antibody concentration, 1 mg/ml) prior to addition of the antibody to the lyophilized oligonucleotides (PLUS and MINUS probes). Incubation with oligonucleotides proceeded overnight at room temperature, followed by addition of 2 μl of ProbeMaker Stop Reagent and incubation for 30 min at room temperature to conclude the labeling reactions. Unreacted oligonucleotides were rendered inactive during this step, preventing spurious signals from being generated. For storage of the antibody-oligonucleotide conjugates, 24 μl ProbeMaker storage buffer was added. The final concentration of the antibody-oligonucleotide conjugates were ~0.4 mg/ml and stored at 4^{o} C until use.

4.8. *In situ* proximity ligation assay

Cultured cells were plated onto 8-well chamber slides (Millipore) in media for one day prior to stimulation as described above. Cells were stimulated for 0, 5, 10, or 60 min with PRL, washed twice in PBS, then fixed in 4% paraformaldehyde for 10 min. Fixed cells were subsequently washed twice with PBS, dried and frozen at -20^{o} C.

On the day of the experiment, slides were thawed at room temperature and rehydrated in PBS for 10 min at room temperature. All steps of the Duolink protocol were performed as open droplet reactions on the chamber slides, using 30 μl volume per chamber to ensure complete coverage of the cells. Cells were then permeabilized in PBS+0.1% Triton X-100 for 10 min at room temperature, washed twice in PBS, and blocked in 1X Duolink Blocking

solution for 30 min at 37° C in a humidity chamber to prevent evaporation. PRLR primary antibody-oligonucleotide conjugates were diluted in PLA Probe Diluent to 5 μg/ml, and applied to slides overnight at 4° C in a cooled humidity chamber. On the second day, slides were washed 3 times in 1X Duolink Wash Buffer A to remove excess antibody-oligonucleotide conjugates. Bound antibody-oligonucleotide conjugates were ligated together for 30 min at 37° C according to the manufacturer's instructions. Subsequently, ligated templates were amplified for 2 hr at 37° C according to the manufacturer's protocol, washed twice for 10 min in Duolink 1X Wash Buffer B, and once for 1 min in 0.1X Wash Buffer B prior to mounting with Duolink Fluorescence mounting media (which also contains DAPI for nuclear counterstaining) and observation under a fluorescent microscope.

Image acquisition was performed using a Zeiss Axioscope M1 under 40X magnification and an AxioCam HR. Image analysis was performed using the Duolink ImageTool software according to the instructions provided by OLINK®.

5. Results

5.1. Characterization of PRLR isoform specific monoclonal antibodies

We have recently prepared and characterized PRLR isoform specific polyclonal antibodies [5]. However, a limitless source of polyclonal antibody is restricted because it is generated by repeated immunization of a rabbit. Each antibody preparation has the potential to vary in its specificity as well. Monoclonal antibodies are more homogeneous and can produce a near inexhaustible supply of reagent. We used the same peptide sequence as for the preparation of isoform specific polyclonal antibodies and, again, demonstrate specificity for the individual isoforms. CHO cells were transiently transfected with cDNA containing the individual PRLR isoforms; western blot analysis from cell lysates indicate that the antibodies detect the corresponding protein without cross-reactivity (Figure 1A).

By immunocytochemical analysis using transiently transfected CHO cells, we were able to positively stain for isoform specific PRLR. As shown in Figure 1B, no cross-reactivity was identified using the antibodies on cells transfected with non-corresponding PRLR cDNA. By both western and immunochemical analysis we were able to demonstrate the specificity of the PRLR isoform specific monoclonal antibodies.

5.2. Immunofluorescent staining of human breast tissue

Once we determined the specificity of the isoform specific monoclonal antibodies on transfected cells, we tested them on histosections obtained from reduction mammoplasty specimens. In order to examine the localization patterns of the PRLR, we stained the tissues simultaneously with LF and either SF1a or SF1b antibodies. Similar, striking, distribution of isoform expression was observed, regardless of whether paraffin-embedded or frozen sections were used. As seen in Figure 2, LF expression appeared primarily basal, whereas SF localized more luminally.

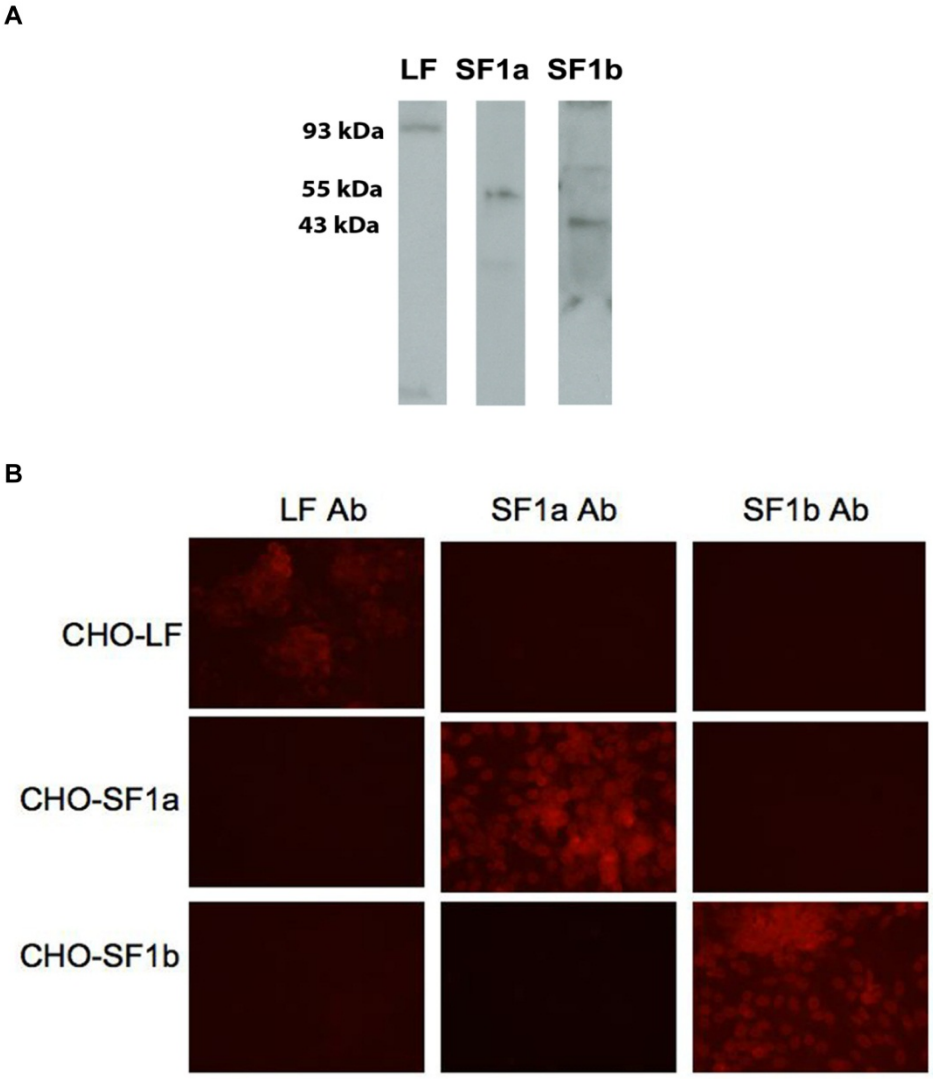

Figure 1. Characterization of PRLR isoform antibodies. **A**. Western blot analysis indicating specificity of monoclonal antibodies. CHO cells were transiently transfected with isoform specific PRLR cDNA as described. Cell lysates were prepared and proteins separated by PAGE. Each isoform specific lysate was probed with each isoform specific antibody. Western blot analysis was performed twice with separate lysates. Data shown are a representative autoradiogram. Molecular weights are marked as indicated: LF = 93kDa, SF1a = 55kDa, SF1b = 43kDa. **B**. Fluorescent immunocytochemical analysis. CHO cells were transiently transfected with isoform specific PRLR cDNA as described. Specific staining was observed. The negative control lacks primary antibody. Data shown are representative of triplicate experiments. Magnification 20X.

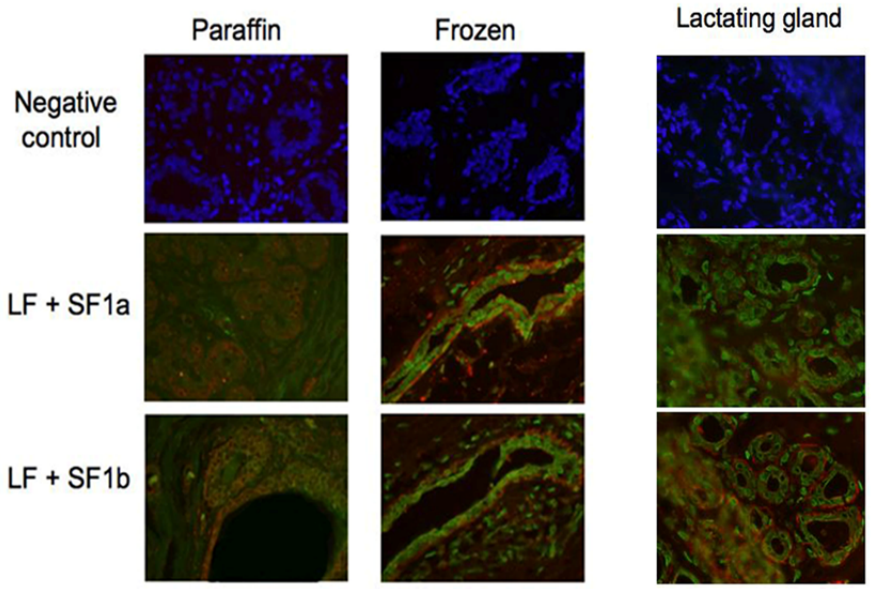

Figure 2. Fluorescent immunohistochemical analysis from normal breast tissues. Representative photos taken from breast reduction mammoplasty specimens. Images in left panels are taken from paraffin embedded tissues; middle panels are imaged from frozen sections; right panels are taken from paraffin embedded normal lactating mammary tissues. Negative control indicates no primary antibody used. LF is indicated by green fluorescence; SF is indicated by red fluorescence. LF = long form; SF = short form. Magnification 40X.

However, the expression patterns localized quite differently in cancer tissue. The PRLR isoforms appeared to colocalize, but were only present in specific areas (Figure 3). The pattern seemed more random, concentrated in "hot spots," particularly for SF1a.

5.3. *In situ* proximity ligation assay monitors PRLR dimerization

The Duolink reagents allow for specific protein-protein interactions to be examined *in situ*. Using antibodies to PRLR-LF, SF1a and SF1b we generated PRLR isoform-specific PLA probes in order to monitor every possible dimer combination using the OLINK ProbeMaker kit. This kit allows for the direct conjugation of the oligonucleotide (PLUS or MINUS end) to the primary antibody, which is essential for examining homodimers. Using these probes, we examined the six possible dimer pairings (LF/LF, SF1a/SF1a, SF1b/SF1b, LF/SF1a, LF/SF1b, SF1a/SF1b) in six established breast cancer cell lines: T47D, ZR75-1, MDA-MB-231, MDA-MB-468, MCF7, and SK-BR-3 in the absence and presence of PRL stimulation. In addition to the specific antibodies, we included non-specific isotyped control antibodies as negative controls (i.e. LF/NSR, where NSR is a non-specific rabbit IgG in place of a specific rabbit antibody against PRLR). After the proximity ligation reaction has taken place, a single fluorescent red dot is observed. This dot represents a single molecular interaction between the two proteins being interrogated.

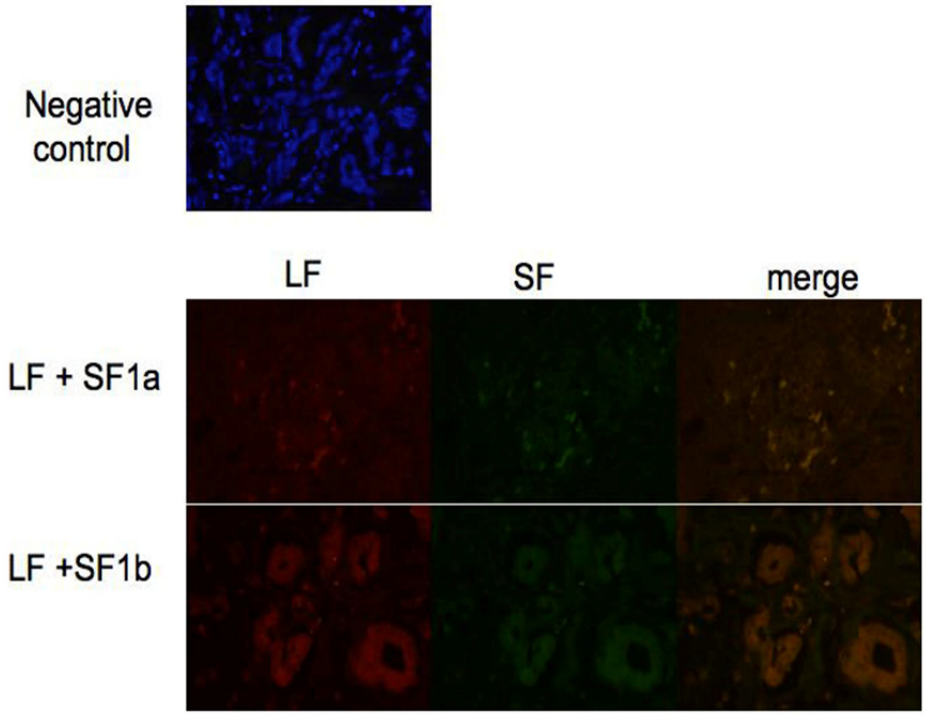

Figure 3. Fluorescent immunohistochemical analysis from breast cancer tissues. Representative photos taken from breast tumor specimens. LF is indicated by green fluorescence; SF is indicated by red fluorescence. LF = long form; SF = short form. Magnification 40X.

With the exception of the MDA-MB-231 cells, similar patterns of expression were observed in all breast cell lines tested. In the ER positive MCF7 cells, dimers of all six potential combinations were observed in the absence of stimulation, and were maintained throughout the stimulation with PRL (Figure 4A). However, in the ER negative MDA-MB-231 cells, a much more complex pattern appeared (Figure 4B). We observed changes in the levels of several dimers over the course of PRL stimulation, suggesting that the different dimer pairings may be utilized by the cell to mitigate responses to prolonged PRL stimulation.

While performing these experiments, we noticed a significant amount of PRLR dimers at either the perinuclear or nuclear region of the cell. Several receptors in the mammary gland have been shown to undergo nuclear translocation including EGFR, FGFR, and GHR [13]. However, there is little information known about the nuclear localization of PRLR. Several reports in the literature have offered contradicting evidence for PRLR nuclear translocation [19-21].

In a preliminary study of PRLR isoform nuclear translocation, MDA-MB-231 cells were stimulated with PRL

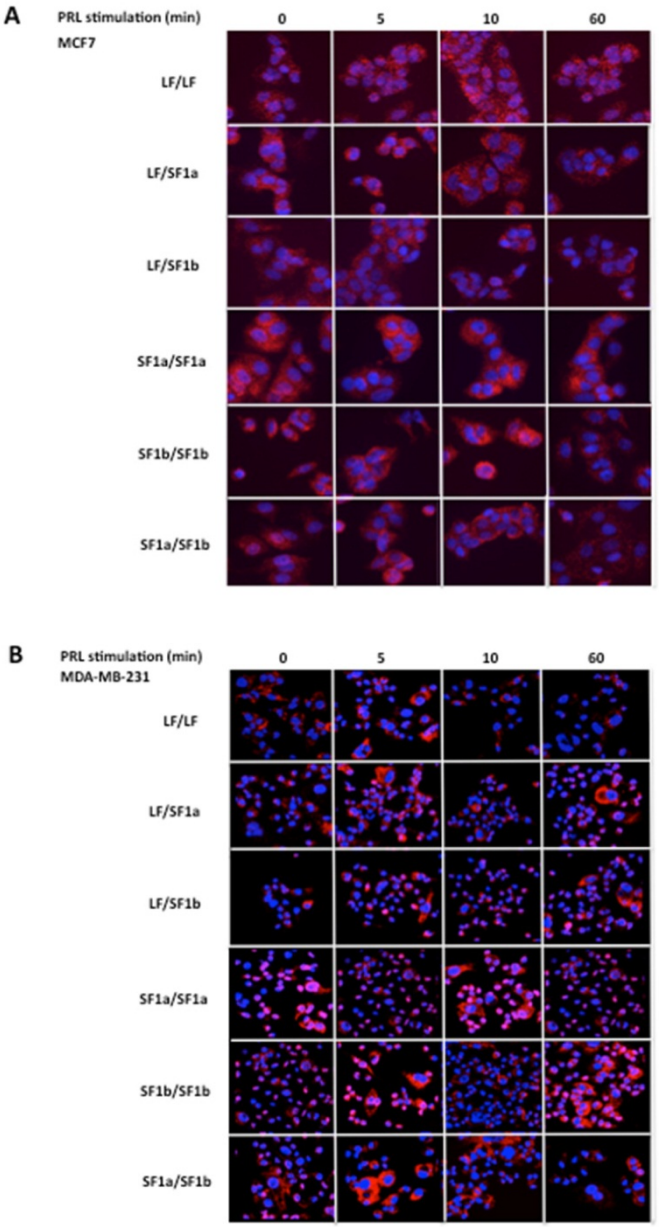

Figure 4. Duolink analysis of breast cancer cell lines for PRL-dependent PRLR dimerization. Representative images are shown for each dimer pairing in both MCF7 (panel A) and MDA-MB-231 (panel B) cells at 0, 5, 10 and 60 min post-stimulation with PRL. Magnification 40X. Nuclei stained (shown in blue) with DAPI, Duolink signal shown in red. Each red dot represents a single dimerization event.

6 hr prior to Duolink analysis to examine steady-state nuclear localization of PRLR dimer formation using confocal microscopy (Figure 5). Of the various combinations of PRLR isoform dimers that were examined, nearly all exhibited some nuclear localization. The exception was for SF1a/SF1a homodimers, which formed perinuclear rings but showed little to no nuclear localization (Figure 5B). Homodimers of the two short forms or a heterodimer of the two short forms (Figure 5B, SF1a/SF1a; Figure 5C SF1b/SF1b; Figure 5D, SF1a/SF1b) exhibited significantly higher levels of nuclear localization while LF homodimers (Figure 5A) and the two LF-short form heterodimers (Figure 5E, LF/SF1a; Figure 5F, LF/SF1b) showed modest levels of nuclear localization. These results confirm that nuclear localization exists for the human prolactin receptor isoforms and may suggest a new role for them as potential transcriptional regulators. Pathways indicating the intranuclear transport and function of PRL and its receptor targeting intracellular actions, such as transcription, have been demonstrated [13]. Increases in transcription may effect cell proliferation and/or differentiation. However, the function of perinuclear localization has yet to be explored.

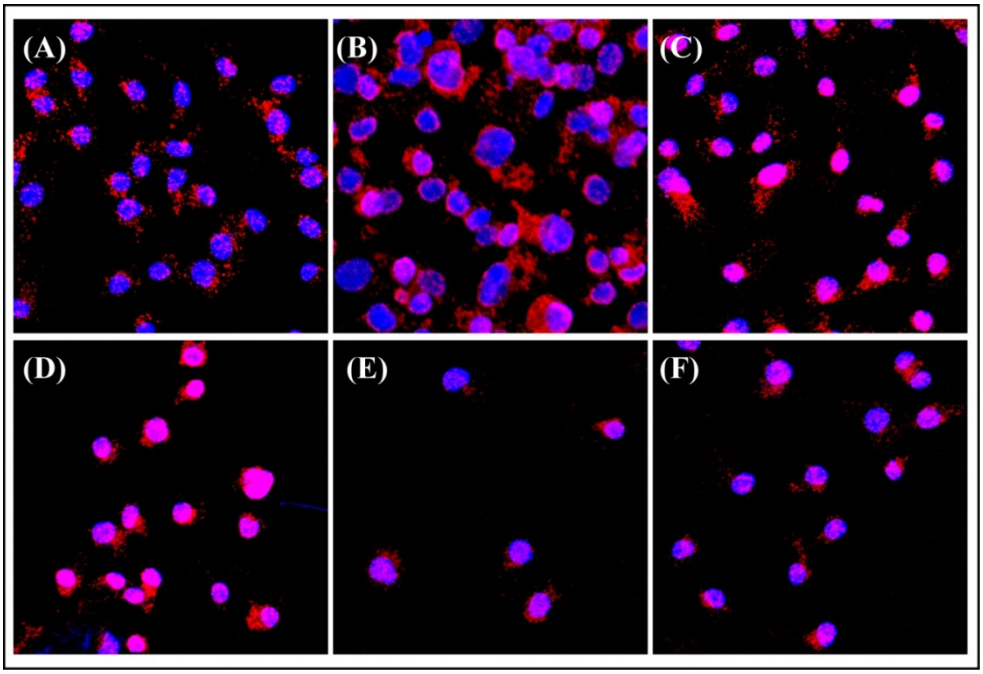

Figure 5. PRLR isoform dimers exhibit different localization patterns. MDA-MB-231 cells were stimulated for 6 hr with 500 ng/ml recombinant human PRL, fixed and examined by confocal microscopy for PRLR dimer localization using Duolink. Dimer combinations: A. LF/LF; B. SF1a/SF1a; C. SF1b/SF1b; D. SF1a/SF1b; E. LF/SF1a; F. LF/SF1b. Images were acquired using a 20X objective with a 2X zoom.

6. Discussion and further research

Prolactin signaling through the LF of the PRLR has been well studied [13]. Two short forms of the PRLR (SF1a and SF1b) share common extracellular and transmembrane domains with the LF, yet contain different cytoplasmic sequences due to alternative splicing of exon 11 [1,2]. The role of these short forms in PRLR function remains elusive, in part due to a lack of specific reagents. Both SF1a and SF1b contain the Box1 binding site for Jak2 and MAPK proteins, yet lack the Box 2 site (and downstream phosphorylation sites) required for STAT binding [2, 14]. By lacking part of intracellular signaling domain, the short forms of the PRLR act as dominant negatives of the LF in transfected cells and its effects most likely occur through heterodimerization with LF [5]. While both short forms can function as a dominant negative, SF1b is the more potent negative regulator of LF function.

To facilitate the study of the PRLR short forms, we generated isoform-specific polyclonal antibodies and demonstrated a breast cancer specific pattern of expression. While all tumor biopsies expressed both LF and SF1b equally, the presence of SF1a was detected mainly in ductal breast carcinoma biopsies and not in those derived from lobular carcinomas [5]. These data suggest diagnostic potential for the PRLR short forms.

The mere expression profiles of these proteins may not serve as sufficient biomarkers, as PRLR dimers are the functional unit for PRL-mediated events. Therefore, an analysis of the ratios of the various potential dimers may be needed to generate a more complete understanding of PRLR signaling. Techniques such as BRET and FRET have been used to examine PRLR dimer formation [14-17]. However, these techniques collectively constrain the user to cells that express tagged constructs and prevent analysis of tissue samples. Co-immunoprecipitation has been used with moderate success for PRLR dimer analysis and avoids the need for tagged constructs, but lacks quantitation, requires specific antibodies, and is devoid of any cellular localization information. To overcome these technical challenges, we employed an *in situ* proximity ligation assay developed by OLINK®. This technique allows for the sensitive detection of protein-protein interactions in unmodified cells and tissue. Using the newly generated rabbit and mouse monoclonal PRLR isoform-specific antibodies, we examined PRLR dimer formation in breast cancer cell lines in the absence and presence of PRL stimulation. Due to the flexibility of the method, we were able to monitor all possible homo- and hetero-dimers concurrently.

We were able to confirm that PRLR homo- and hetero-dimers form in the absence of PRL, similar to reports by others [14, 17]. Similar reports have shown that members of the EGFR family can form dimers in the absence of ligand [18]. In total, we observed homodimers of LF/LF, SF1a/SF1a, and SF1b/SF1b and heterodimers of LF/SF1a, LF/SF1b, and SF1a/SF1b in two different, but well-established breast cancer cell lines, MCF7 and MDA-MB-231. While SF homodimerization has been shown, heterodimerization of the short forms has been examined but not proven [16]. However, these assays utilized PRLR receptors C-terminally tagged with GFP or Rluc to perform BRET analysis, which may somehow block the detection of the SF heterodimer. The functional consequence of the SF1a/SF1b heterodimer is not known. Given that both short forms lack the majority of the intracellular domain, this

dimer may be formed to limit the inhibitory activity of each monomer towards the LF by a yet-to-be discovered mechanism.

In addition to confirming the existence of all possible dimer pairings, we were able to show that the different PRLR dimers peaked at different times during the PRL time course. These data suggest that upon stimulation with PRL, regulatory events occur within the cell to favor a particular signaling outcome. For example, an increase in LF/SF1b dimers is predicted to sequester otherwise functional LF monomers into inactive dimers with SF1b. These dimers (and similarly LF/SF1a dimers) would be capable of binding PRL, but would most likely be unable to transmit the signal from ligand binding to the intracellular milieu. Thus, the dominant negative nature of the PRLR short forms could occur by isolating PRLR LF monomers and also result in diminished effects of PRL on cells. Further studies would be required to better understand the dimerization time course for PRLR in these and other breast cancer cell lines.

The confirmation of the nuclear localization of PRLR dimers is an important finding. Conflicting reports were found in the literature [13, 19, 20], however our study confirms that PRLR dimers can be found in the nucleus of cultured breast cancer cells. Interestingly, the amount of nuclear localized PRLR was different for the various dimer pairings tested in MDA-MB-231 cells. In general, the SF dimer combinations (SF1a/SF1a, SF1a/SF1b, and SF1b/SF1b) exhibited higher levels of nuclear localization than dimers containing at least one monomer of LF. In addition, only SF1a homodimers localized to a perinuclear region, and appeared as rings around the nucleus. Together these data suggest a potential transcriptional role for PRLR. Recent work performed in the Walker laboratory [21] demonstrated that, in prostate cancer, the expression of SF1b was upregulated after treatment with the PRL inhibitor S179D. This increase in repression also led to an upregulation of p21 and the vitamin D receptor (VDR), both known to affect differentiation and apoptosis. *In vitro* studies also confirmed that long-term overexpression to SF1b decreased the growth and migration of prostate cancer cells, in addition to enhancing cell-matrix interactions and cell-cell aggregation [22]. Abnormalities in the vitamin D endocrine system have been linked to many disorders, including cancer [23]. Strong epidemiological associations were made between vitamin D deficiency and breast and prostate cancers. The VDR system may arrest the tumor cell cycle at G1/G0 through several mechanisms such as by induction of p21 gene transcription [24] or by inducing the synthesis and/or stabilization of p27 [25]. Recent work in tumor-derived endothelial cells has implicated VDR as an anti-proliferative factor inducing cell cycle arrest in G1/G0 and tumor angiogenesis [26]. Loss of VDR in this system or in mammary epithelial cells may affect differentiation and apoptosis or modulate intracellular signaling routes. These changes in the tumor microenvironment could potentially result in aberrant angiogenic signaling pathways, possibly even enhancing angiogenesis for a more efficient delivery of chemotherapeutic drugs. PRL and its signaling pathways could be exploited to search for more effective therapies in prostate and breast cancer [27]. Potential synergy with various chemotherapeutics may be another aspect of the importance of dimerization and localization of PRL and its receptors in breast cancer.

As discussed herein, our laboratory has recently published the utility of PRLR isoform-specific antibodies in characterizing breast cancer samples as either lobular or ductal in nature [5]. The generation of monoclonal antibodies to the various PRLR isoforms provides a more renewable and reliable supply of these antibodies, and were crucial to the dimerization studies. To our knowledge, this is the first time that the Duolink *in situ* proximity ligation assay enabled detection of all possible PRLR dimer combinations. The technique is robust, quantitative and relatively easy to use.

With the advent of the tissue microarray (TMA) [28, 29], researchers are able to examine large populations of tissues from patients on a single glass slide. There are many commercially available TMAs as well, including arrays for breast cancer patients. These arrays have typically been evaluated for ER/PR/HER2 status and, in many cases, have both normal and diseased tissue for each patient. Given that OLINK® provides a Brightfield Duolink kit, several studies could be envisioned. First, since the Duolink assay can also be used to obtain quantitative total expression of a target, the application of this technique to TMAs would provide a significantly better means of analyzing the expression levels of targets (rather than high, medium, and low expression). These data could also be combined with expression profiles of the PRLR dimer complexes and ultimately compared with other markers to identify more specific breast cancer signatures. Further correlations could be made with the levels of the hormone PRL itself, which could help further diagnose patients.

The "hormonal responsiveness" of breast cancer has been known for a long time. Unfortunately, this phrase has only been used to indicate responsiveness to estrogen (E) and progesterone (P). However, several other hormones including PRL, growth hormone, and thyroid hormone have been shown to play roles in normal breast development and function and their various roles in breast cancer are being investigated. The complex interplay of the three major hormones involved in normal breast development, E, P, and PRL, is well documented. In model systems that include human breast cancer cells in culture as well as rodent models, E, P, and PRL have all been shown to stimulate growth. In fact, when compared directly with E acting on MCF-7 human breast cancer cells, PRL is a more potent mitogen than E [8].

Additionally, these model systems have demonstrated that each of these hormones acts as more than just a mitogen. Complex systems of inter-regulation exist between these steroids, PRL and their receptors. PRL stimulates growth through both an endocrine as well as an autocrine/paracrine mechanism. The expression of autocrine PRL in human breast cancer cells is regulated by E through action on the PRL promoter [30]. Expression of the PRL gene is regulated by two promoters, the proximal promoter utilized primarily in the pituitary and the distal promoter utilized in breast cancer cells. E directly induces hPRL gene expression in T47D human breast cancer cells through the action of a functional non-canonical E response element (ERE) and an AP1 site on the distal promoter. Both the ERE and AP1 sites are required for full induction of promoter activity through the alpha form of the ER.

Similarly, the interplay of P and PRL is well established in various models. PR and PRLR are co-expressed temporally and spatially in the developing mouse mammary gland. In

mammary glands from ovariectomized female mice lacking both E and P, neither P nor PRL stimulate DNA synthesis in epithelial or adjacent stromal cells. However, simultaneous injection of P and PRL results in a significant synergistic effect on DNA synthesis in both cell types [31]. Similarly, disruption of expression and distribution of PR in the mammary gland results in a parallel disruption of expression and distribution of the PRLR suggesting inter-regulation of these receptors [32]. Expression of the PRLR in human cells is regulated through a complex system of promoters. The PRLR gene in humans has six exon 1s, the most generic of which (PRLR promoter region III) is functional in human breast cancer cells. T47D human breast cancer cells treated with P overexpress the PRLR and activate PRLR promoter III. This promoter lacks a classical P response element. Thus P acts through the cooperative interaction of the PR with the transcription factors C/EBP and an adjacent Sp1A site to confer P responsiveness leading to increased expression of the PRLR [33].

These examples of the complex interactions of E, P, and PRL underscore the importance of understanding all three hormones' actions and their receptor interactions, distribution, and functions in the normal human breast and in breast cancer. Effective tools for these studies are now available.

7. Conclusion

Just as the identification of the ER and PR are now routinely performed on all clinical breast cancer samples, screening for PRLR status and isoform profile may also one day become a routine procedure in the characterization of breast cancers. Isoform specific antibodies to the PRLR can be powerful tools in detection and characterization of breast and other cancers and provide valuable insights into the important PRLR signaling pathways that could be effective targets for prevention and treatment.

Author details

Erika Ginsburg, Christopher D. Heger, Paul Goldsmith and Barbara K. Vonderhaar
Center for Cancer Research, National Cancer Institute, National Institutes of Health, USA

Acknowledgement

This research was supported by the Intramural Research Program of the NIH, National Cancer Institute. We thank Sarah J. Tarplin for her assistance with the immunostaining and to Dr. Jodie M. Fleming for helpful discussions. The authors have no competing interests.

8. References

[1] Trott JF, Hovey RC, Koduri S, Vonderhaar BK (2003) Alternative splicing to exon 11 of human prolactin receptor gene results in multiple isoforms including a secreted prolactin-binding protein. *J Mol Endocrinol* 30(1):31-47.

[2] Hu ZZ, Meng J, Dufau ML (2001) Isolation and characterization of two novel forms of the human prolactin receptor generated by alternative splicing of a newly identified exon 11. *J Biol Chem* 276(44):41086-41094.

[3] Clevenger CV, Furth PA, Hankinson SE, Schuler, LA (2003) The role of prolactin in mammary carcinoma. *Endocrine Rev* 24(1): 1-24.

[4] Meng J, Tsai-Morris CH, Dufau ML (2004) Human prolactin receptor variants in breast cancer: low ratio of short forms to the long-form human prolactin receptor associated with mammary carcinoma. *Cancer Res* 64(16):5677-5682.

[5] Ginsburg E, Alexander S, Lieber S, Tarplin S, Jenkins L, Pang L, Heger CD, Goldsmith P, Vonderhaar BK (2010) Characterization of ductal and lobular breast carcinomas using novel prolactin receptor isoform specific antibodies. *BMC Cancer* 10:678.

[6] Hankinson SE, Wilett WC, Michaud DS, Manson JE, Colditz GA, Longcope C, Rosner B, Speizer FE (1999) Plasma prolactin levels and subsequent risk of breast cancer in postmenopausal women. *J Natl Cancer Inst* 91:629-634.

[7] Tworoger SS, Eliassen AH, Sluss P, Hankinson SE (2007) A prospective study of plasma prolactin concentration and risk of premenopausal and postmenopausal breast cancer. *J Clin Oncol* 25(12):1482-1488.

[8] Biswas R, Vonderhaar, BK (1987) Role of serum in prolactin responsiveness of MCF-7 human breast cancer cells in long term tissue culture. *Cancer Res* 47:3509-3514.

[9] Faupel-Badger JM, Ginsburg E, Fleming JM, Susser L, Doucet T, Vonderhaar BK (2010) 16-kDa prolactin reduces angiogenesis, but not growth of human breast cancer tumors in vivo. *Horm Canc* 1(2):71-79.

[10] Gill S, Peston D, Vonderhaar BK, Shousha S (2001) Expression of prolactin receptors in normal, benign and malignant breast tissue: an immunohistological study. *J Clin Pathol* 54(12):956-960.

[11] Bonneterre J, Peyrat JP, Vandewalle B, Beuscart R, Vie MC, Cappelaere P (1982) Prolactin receptors in human breast cancer. *Eur J Cancer Clin Oncol* 18:1157-1162.

[12] Bradford MM (1976) A rapid and sensitive method for the quantitation of microgram quantities of protein utilizing the principle of protein-dye binding. *Anal Biochem* 72:248-254.

[13] Clevenger CV (2003) Nuclear localization and function of polypeptide ligands andtheir receptors: a new paradigm for hormone specificity within the mammary gland? *Breast Cancer Res* 5:181-187.

[14] Qazi AM, Tsai-Morris CH, Dufau ML. Ligand-independent homo- and heterodimerization of human prolactin receptor variants: inhibitory action of the short forms by heterodimerization. *Mol Endocrinol* 2006;20(8):1912–1923.

[15] Biener E, Martin C, Daniel N, Frank SJ, Centonze VE, Herman B, Djiane J, Gertler A (2003) Ovine placental lactogen-induced heterodimerization of ovine growth hormone and prolactin receptors in living cells is demonstrated by fluorescence resonance energy transfer microscopy and leads to prolonged phosphorylation of signal transducer and activator of transcription (STAT) 1 and STAT3. *Endocrinology* 144(8): 3532-3540.

[16] Tan D, Johnson DA, Wu W, Zeng L, Chen YH, Chen WY, Vonderhaar BK, Walker AM (2005) Unmodified prolactin (PRL) and S179D PRL-initiated bioluminescence resonance

energy transfer between homo- and hetero-pairs of long and short human PRL receptors in living cells. *Mol Endocrinol* 19(5): 1291-1303.

[17] Gadd SL, Clevenger CV (2006) Ligand-independent dimerization of the human prolactin receptor isoforms: functional implications. *Mol Endocrinol* 20(11) 2734-2746.

[18] Yu X, Sharma KD, Takahashi T, Iwamoto R, Mekada E (2002) Ligand-independent dimer formation of epidermal growth factor receptor (EGFR) is a step separable from ligand-induced EGFR signaling. *Mol Biol Cell* 13(7): 2547-2557.

[19] Perrot-Applanat M, Gualillo O, Buteau H, Edery M Kelly, PA (1997) Internalization of prolactin receptor and prolactin in transfected cells does not involve nuclear translocation. *J Cell Sci* 110:1123-1132.

[20] Rao YP, Buckley DJ, Buckley, AR (1995) The nuclear prolactin receptor: a 62- kDa chromatin-associated protein in rat Nb2 lymphoma cells. *Arch Biochem Biophys* 322:506-515.

[21] Wu W, Ginsburg E, Vonderhaar BK, Walker AM (2005) S179D prolactin increases vitamin D receptor and p21 through up-regulation of short 1b prolactin receptor in human prostate cancer cells. *Cancer Res* 65(16):7509-7515.

[22] Huang KT, Walker AM (2010) Long term increased expression of the short form 1b prolactin receptor in PC-3 human prostate cancer cells decreases cell growth and migration, and causes multiple changes in gene expression consistent with reduced invasive capacity. *Prostate* 70(1):37-47.

[23] Dusso AS, Brown AJ, Slatopolsky E (2005) Vitamin D. *Am J Physiol Renal Physiol* 289:F8-F28.

[24] Liu M, Lee M-H, Cohen M, Bommakanti M, Freedman LP (1996) Transcriptional activation of the cdk inhibitor p21 by vitamin D3 leads to the induced differentiation of the myelomonocytic cell line U937. *Genes & Dev* 10:142-153.

[25] Li P, Li, C, Zhao X, Zhang X, Nicosia SV (2004) p27 ^{kip1} stabilization and G_1 arrest by 1,25-dihydroxyvitamin D_3 in ovarian cancer cells mediated through down-regulation of cyclin E/cyclin-dependent kinase 2 and skp1-cullin-F-box protein/skp2 ubiquitin ligase. *J Biol Chem* 279(24): 25260-25267.

[26] Chung I, Han G, Seshadri M, Gillard BM, Yu W, Foster BA, Trump DL, Johnson CS (2009) Role of vitamin D receptor in the antiproliferative effects of calcitrol in tumor-derived endothelial cells and tumor angiogenesis in vivo. *Cancer Res* 69(3): 967-975.

[27] Jacobson EM, Hugo ER, Borcherding DC, Ben-Jonathan N (2011) Prolactin in breast abd prostate cancer : Molecular and genetic perspectives. *Discov Med* 11(59):315-324.

[28] Battifora H, Mehta P (1990) The checkerboard tissue block. An improved multitissue control block. *Lab Invest* 63:722-724.

[29] Kononen J, Bubendorf L, Kallioniemi A, Barlund M, Schraml P, Leighton S, Torhorst J, Mihatsch MJ, Sauter G, Kallioniemi OP (1998) Tissue microarrays for high-throughput molecular profiling of tumor specimens. *Nat Med* 4:844-847.

[30] Duan R, Ginsburg E, Vonderhaar BK (2008) Estrogen stimulates transcription from the human prolactin distal promoter through AP1 and estrogen responsive elements in T47D human breast cancer cells. *Mol Cell Endocrinol* 281(1-2):9-18.

[31] Hovey RC, Trott JF, Ginsburg E, Sasaki MM, Fountain SJ, Sundararajan K, Vonderhaar BK (2001) Transcriptional and spatiotemporal regulation of prolactin receptor mRNA and cooperativity with progesterone receptor function during ductal branch growth in the mammary gland. *Dev Dyn* 222(2):192-205.

[32] Grimm SL, Seagroves TN, Kabotyanski EB, Hovey RC, Vonderhaar BK, Lydon JP, Miyoshi K, Hennighausen L, Ormandy CJ, Lee AV, Stull MA, Wood TL, Rosen JM (2002) Disruption of steroid and prolactin receptor patterning in the mammary gland correlates with a block in lobuloalveolar development. *Mol Endocrinol* 16(12):2675-2691.

[33] Goldhar AS, Duan R, Ginsburg E, Vonderhaar BK (2011) Progesterone induces expression of the prolactin receptor gene through cooperative action of Sp1 and C/EBP. *Mol Cell Endocrinol* 335(2):148-157.